

AC properties of 2D percolation networks: a transfer matrix approach

This article has been downloaded from IOPscience. Please scroll down to see the full text article.

1986 J. Phys. A: Math. Gen. 19 3153

(<http://iopscience.iop.org/0305-4470/19/15/036>)

View [the table of contents for this issue](#), or go to the [journal homepage](#) for more

Download details:

IP Address: 129.252.86.83

The article was downloaded on 31/05/2010 at 19:22

Please note that [terms and conditions apply](#).

AC properties of 2D percolation networks: a transfer matrix approach

J M Laugier†, J P Clerc†, G Giraud† and J M Luck‡

† Département de Physique des Systèmes Désordonnés, Université de Provence, Centre de St Jérôme, 13397 Marseille Cedex 13, France

‡ Service de Physique Théorique, CEN Saclay, BP2, 91191 Gif-sur-Yvette Cedex, France

Received 2 December 1985, in final form 11 February 1986

Abstract. The frequency dependent AC properties of 2D random resistor–capacitor mixtures are studied through a numerical transfer matrix method. Our algorithm, which generalises to the complex impedances used by Herrmann *et al*, permits a detailed study of the scaling laws obeyed by the complex dielectric constant in the critical regime (low frequency and concentration close to the geometrical percolation threshold). The duality property of the system is extensively used throughout our analysis. Quantities of experimental interest, such as the loss angle δ and the Cole and Cole plot of the dielectric constant, are also examined, both close to and away from the critical point.

1. Introduction

This paper is devoted to the frequency dependent (complex) conductivity of conductor–insulator random mixtures. As usual, we model such systems by a percolation problem on a lattice, where each bond is conducting (resistance R_0) with probability p and insulating (capacitance C_0) with probability $(1-p)$ (Webman *et al* 1975, Efros and Shklovskii 1976). Since each capacitance has an impedance $(iC_0\omega)^{-1}$ at frequency $\omega/2\pi$, the frequency dependent conductivity $\Sigma(p; \omega)$ of the system only depends on ω/ω_0 , where $\omega_0^{-1} = R_0C_0$ is a microscopic timescale.

The quantity $\Sigma(p; \omega)$ is the ‘density’ of complex admittance (inverse impedance) of the model on a macroscopic scale, which generalises the usual notion of DC conductivity to AC properties. This model interpolates between two well known limits. At zero frequency the capacitances are perfect insulators and the conductivity of this conductor–insulator mixture is zero whenever p is smaller than the bond percolation connectivity threshold p_c and behaves like $\Sigma \sim AR_0^{-1}(p-p_c)^t$ for $p \rightarrow p_c^+$. Conversely, at infinite frequency, the situation is equivalent to that of a normal superconductor mixture with a fraction $q=1-p$ of perfectly conducting bonds: the conductivity diverges as $\Sigma \sim (p_c - q)^{-s}$ when $q \rightarrow p_c$.

In the critical region, where both $(p-p_c)$ and ω/ω_0 are small, the conductivity $\Sigma(p; \omega)$ (of the infinite system) has been suggested to obey the following scaling behaviour:

$$\Sigma(p; \omega) = R_0^{-1} |p - p_c|^t \Phi_{\pm} \left(\frac{i\omega}{\omega_0} |p - p_c|^{-s-t} \right) \quad (1)$$

where the subscript \pm refers to the sign of $(p-p_c)$ (Webman *et al* 1975, Efros and Shklovskii 1976, Straley 1976, 1977).

This scaling law has been justified by Stephen (1978) within a field-theoretical approach and an $\varepsilon = 6 - d$ expansion. The situation is quite similar to that of Φ^4 theory with respect to usual static critical phenomena. In particular, the complex scaling functions Φ_{\pm} are expected to be regular and universal, up to scale fixing. Moreover, Σ is regular in p at fixed non-zero frequency. Therefore, when their argument is large, both scaling functions are asymptotic to

$$\Phi_{+}(ix) \sim \Phi_{-}(ix) \sim K(ix)^u$$

where K is some real constant and hence

$$\Sigma(p_c; \omega) \simeq R_0^{-1} K e^{i\pi u/2} (\omega/\omega_0)^u \quad (2)$$

for $\omega \ll \omega_0$. The universal exponents s , t , u are related through

$$u = t/(s + t). \quad (3)$$

The power-law behaviour (2) at the percolation threshold has the following remarkable outcome: the loss angle δ , commonly defined by

$$\tan \delta = \text{Re } \Sigma / \text{Im } \Sigma \quad (4)$$

assumes the *universal* value

$$\delta_c = \frac{\pi}{2} \frac{s}{s + t} = \frac{\pi}{2} (1 - u) \quad (5)$$

at $p = p_c$ and low frequency. This result, which clearly involves no adjustable parameter, is a simple consequence of the scaling law (1); it seems to have been pointed out only recently (Clerc *et al* 1984, 1985, Luck 1985). The loss angle has been measured in two different experimental situations: mixtures of powders (Laugier 1982) and micro-emulsions (van Dijk 1985). The agreement with (5) in the critical region is satisfactory: this provides a good check of the validity of the modelling of these materials by percolation networks. Up to now, the available quantitative studies of the AC conductivity in two and three dimensions have dealt with real space renormalisation group methods (Wilkinson *et al* 1983, Luck 1985) or with exact solutions on deterministic inhomogeneous fractals (Clerc *et al* 1984, 1985).

The aim of the present paper is to examine various properties of the conductivity $\Sigma(p; \omega)$, including a detailed study of the critical region, as well as quantities of experimental interest, by a transfer matrix method, which permits a direct treatment of the resistor-capacitor model on regular lattices.

We shall restrict ourselves to the two-dimensional case and use a square lattice. Our method can be easily generalised to other regular lattices in two and higher dimensions.

It is well known that the admittance Y of a macroscopic two-dimensional sample is expressed in the same units as the complex conductivity Σ , since Σ is nothing else than the admittance of a square of arbitrary size. The (geometrical) self-duality of the square lattice implies that the bond percolation threshold p_c is exactly $\frac{1}{2}$, the critical exponents s and t are equal, $u = \frac{1}{2}$, $\delta_c = \pi/4$, and more generally the conductivities at dual frequencies ω and ω_0^2/ω obey an exact duality relation, which can be derived from Straley's (1977) work as follows. This author considers the macroscopic conductivity $\Sigma(p, a; q, b)$ of a random mixture of conductances a and b which occur with probabilities p and $q = 1 - p$, respectively. Making use of simple symmetry and

homogeneity considerations, and of the *geometrical self-duality* of planar graphs, Straley obtains the very general identities:

$$\begin{aligned} \Sigma(p, a; q, b)/(ab) &= \Sigma(p, b^{-1}; q, a^{-1}) \\ &= 1/\Sigma(q, a; p, b) \end{aligned} \tag{6}$$

which will be shown to have remarkable outcomes. If we remember that $\Sigma(p; \omega)$ is a short notation for $\Sigma(p, R_0^{-1}; q, iC_0\omega)$ and use equation (6) with $a = R_0^{-1}$; $b = iC_0\omega$, together with simple real-analyticity properties (Σ is changed into its complex conjugate whenever a and b occur), we easily get the two very convenient expressions:

$$\Sigma(p; \omega)\Sigma^*(p; \omega_0^2/\omega) = R_0^{-2} \tag{7a}$$

$$\Sigma(p; \omega)\Sigma(1-p; \omega) = iR_0^{-1}C_0\omega \tag{7b}$$

where the asterisk denotes complex conjugation. It is clear from their geometrical origin that these remarkable results (equations (6) and (7)) only hold for the conductivity Σ of the *infinite* plane and are *not* valid for the conductivities $\Sigma_n(p; \omega)$ that we shall consider hereafter, just because these are defined on strips with periodic transverse boundary conditions, which are *not* geometrically self-dual objects.

A particularly interesting consequence of self-duality can be derived by inserting the scaling law (1) into equation (7b). We obtain a remarkable identity between both bulk scaling functions Φ_{\pm} , namely

$$\Phi_+(ix)\Phi_-(ix) = ix \tag{7c}$$

where x denotes the scaling variable $x = (\omega/\omega_0)|p - p_c|^{-s-t}$. In particular, the constant K appearing in equation (2) is equal to 1 for our bond percolation clusters on a square lattice.

We have extended to complex admittances the transfer matrix algorithm introduced by Herrmann *et al* (1984). This procedure consists in computing with a very high numerical accuracy the *longitudinal* conductivities $\Sigma_n(p; \omega)$ on strips of infinite length and finite width of n lattice spacings. The extrapolation of these data using finite-size scaling laws has been proved to be one of the most efficient ways of computing the critical exponent s in two and three dimensions. The result of Herrmann *et al* concerning the two-dimensional problem is

$$s/\nu = 0.977 \pm 0.010 \tag{8}$$

while the (purely geometrical) correlation length exponent ν is exactly equal to $\frac{4}{3}$, according to den Nijs' (1979) conjecture.

The exponent ratio t/ν can also be obtained through a transfer matrix approach, which consists in computing the *transverse* conductivities of strips of finite width. This method, introduced by Derrida and Vannimenus (1982) and Derrida *et al* (1984), has been recently used by Zabolitzky (1984); the result of this last author, $t/\nu = 0.973 \pm 0.005$, is fully consistent with (8). Throughout the present paper, we shall use the values $s/\nu = t/\nu = 0.975$ and $\nu = \frac{4}{3}$ for the critical exponents.

Our plan is the following. In § 2 we recall briefly the principles of the transfer matrix method, as well as the predictions of finite-size scaling theory. Section 3 presents our results concerning different aspects of the AC conductivity for all values of p and ω ; we discuss quantities of experimental interest such as the loss angle δ , the dielectric constant and its Cole and Cole (1941) plot in the complex ϵ plane. We study in more detail the critical region; we test accurately the finite-size scaling behaviour of $\Sigma_n(p; \omega)$

which involves three relevant parameters, namely $(p - p_c)$, $i\omega/\omega_0$ and n , and hence two reduced variables, of which one is complex. This study therefore reveals a richness of phenomena which is not present in most transfer matrix calculations. Section 4 contains some concluding remarks. It is suggested that the study of the conductivity at small but non-zero frequency can yield a very precise numerical determination of δ_c , and hence of the exponent u , in three dimensions.

2. Method and theoretical framework

The algorithm we have used is merely an extension to complex admittances of the transfer matrix method used by Herrmann *et al* (1984) in their calculation of the superconductivity exponent s in two and three dimensions. Let us describe it briefly in the two-dimensional case. Consider a strip of finite length L and width n with periodic vertical boundary conditions (in order to minimise finite-size effects). The *longitudinal* conductivity of our resistor-capacitor mixture in such a geometry is computed by the following iterative procedure. For a given frequency $f = \omega/2\pi$, using the standard complex notation, we impose the voltages $V = 0$ on the first vertical row and V_i ($1 \leq i \leq n$) on the L th vertical row (see figure 1). The (complex) intensities I_i which flow through the endpoints of that last row and the voltages V_i are related through a (complex) impedance matrix Z :

$$v_i = \sum_{1 \leq j \leq n} Z_{ij} I_{ij} \tag{9}$$

The rules for updating this impedance matrix are as follows:

(a) addition of a *horizontal* bond of impedance z at line k :

$$Z_{ij} \rightarrow Z_{ij} + \zeta_{ij}^{(H)} \quad \text{with} \quad \zeta_{ij}^{(H)} = z \delta_{ik} \delta_{jk} \tag{10a}$$

(b) addition of a *vertical* bond of impedance z between lines k and l :

$$Z_{ij} \rightarrow Z_{ij} + \zeta_{ij}^{(v)} \quad \text{with} \quad \zeta_{ij}^{(v)} = \frac{-(Z_{ik} - Z_{il})(Z_{kj} - Z_{lj})}{z + Z_{kk} + Z_{ll} - Z_{kl} - Z_{lk}} \tag{10b}$$

(no implicit summation over repeated indices).

The complex conductivity $\Sigma_n(p; \omega)$ of the strip of infinite length and finite width n is then given by the following limit:

$$\Sigma_n(p; \omega) = \lim_{L \rightarrow \infty} L / Z_{ii} \tag{11}$$

which exists, and is independent of the line label i , with probability one. Since the conductivity is a self-averaging quantity, it is not necessary to average Σ_n over different

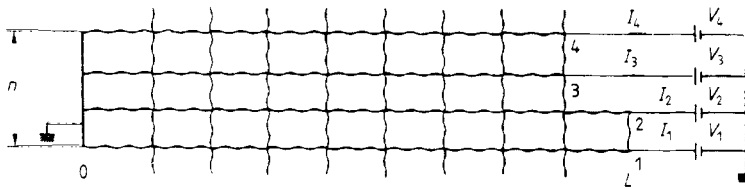


Figure 1. Two-dimensional strip of width n , with periodic boundary conditions in the vertical direction, showing the definition of the voltages V_i and intensities I_i related through the impedance matrix Z .

samples. As the statistical fluctuations around the limit (11) are of order $L^{-1/2}$, it is sufficient to pursue the computation up to a larger value of L in order to diminish the error, which can be roughly estimated by dividing the strip into several parts and comparing the partial results.

The cornerstone of the analysis of our numerical data in the critical region will be the existence of a finite-size scaling law, valid for $|p - p_c| \ll 1$, $\omega \ll \omega_0$ and $n \gg 1$ simultaneously:

$$\Sigma_n(p; \omega) = R_0^{-1} n^{-t/\nu} F\left(\frac{i\omega}{\omega_0} n^{(s+t)/\nu}; (p - p_c)n^{1/\nu}\right). \tag{12}$$

The general validity of the finite-size scaling ‘hypothesis’ formulated by Fisher (1972) has been justified by Brézin (1982) in the context of usual critical phenomena (ϕ^4 theory); it is very likely that it holds in any critical system below its upper critical dimensionality (mean-field-like systems exhibit pathological scaling properties, even in an infinite geometry, such as (apparent) hyperscaling violations). There exist numerous equivalent ways of writing the finite-size scaling law (12). The form we have chosen avoids introducing a singular function.

Let us use the following notation for the arguments of the scaling function $F(ix; y)$

$$x = (\omega/\omega_0)n^{(s+t)/\nu} \quad y = (p - p_c)n^{1/\nu} \tag{13}$$

such that the reduced variables x and y respectively describe the positive half-line and the whole real line in physical situations. Since Σ_n is actually the conductivity of a one-dimensional system, it does not have any singularity in ω or p (except the trivial one-dimensional threshold $p_c = 1$), and hence the scaling function $F(x; y)$ is regular (infinitely differentiable) everywhere, including at $x = y = 0$.

We shall show in § 3 several manifestations of the scaling behaviour (12) in our finite-size data. The bulk scaling law (1) is of course also contained as a limiting case in equation (12), namely, if $x > 0$ and y (real) go to infinity in such a way that $x = \mu|y|^{s+t}$, then (1) is recovered with $F(ix; y) \approx |y|^t \Phi_{\pm}(i\mu)$, where \pm refers to the sign of y . Let us remark that we have lost regularity in y during this procedure. This is not surprising if we remember that all physical quantities are expected to have singularities in the complex p plane which pinch the real axis at the threshold p_c .

3. Numerical results

The numerical results obtained by the transfer matrix method described in § 2 will be presented in terms of the *complex dielectric constant* $\varepsilon(p; \omega)$, defined as usual by

$$\Sigma(p; \omega) = i\omega\varepsilon(p; \omega). \tag{14}$$

The quantities ε_n attached to strips of width n therefore obey the finite-size scaling law:

$$\varepsilon_n(p; \omega) = C_0 n^{s/\nu} G(ix; y) \tag{15}$$

where the scaling functions F and G are simply related through

$$F(ix; y) = ixG(ix; y). \tag{16}$$

First we shall present our results concerning the scaling laws in the critical region, and then discuss the whole ω and p dependence of quantities such as ε and $\tan \delta$, which then have the advantage of being accessible to experimental measurements.

We have used throughout the present work *double precision* complex routines. The data discussed in this paper represent roughly 50 CPU h on the IBM 3081 of CNUSC at Montpellier. Since our method has very good convergence properties outside the critical region (see § 3.2), the essential part of the computer time was spent on the two-variable scaling analysis of § 3.1.

3.1. Scaling in the critical region

We have tested in great detail the finite-size scaling law (15) obeyed by the quantities $\varepsilon_n(p; \omega)$, and extracted the dependence of their scaling function $G(ix; y)$ with respect to its two arguments defined in (13). Consider first the model *at* the percolation threshold of the infinite system. Then $\varepsilon_n(p; \omega)$ depends only on *one* reduced variable:

$$x = \frac{\omega}{\omega_0} n^{(s+t)/\nu}$$

through

$$\varepsilon_n(p_c, \omega) = C_0 n^{t/\nu} G(ix; 0). \quad (17)$$

Moreover, we know *a priori* the limiting behaviour of $G(ix; 0)$ when x goes to zero and infinity. In the first case ($x \rightarrow 0$), the function G is regular:

$$G(ix; 0) = D - iEx + \dots \quad (18a)$$

where D and E are two positive constants. In the $x \rightarrow \infty$ limit, the bulk scaling law (2) is recovered as

$$G(ix; 0) \simeq (ix)^{-1/2} \equiv K^{-1} e^{-i\delta_c} x^{-1/2} \quad (18b)$$

where $K = 1$ and $\delta_c = \pi/4$ are as in equations (2)-(5).

Figures 2 and 3 respectively show plots of the real and (minus) the imaginary part of the scaling function $G(ix; 0)$ against x . The data corresponding to different sizes n collapse onto a single curve. Figure 4 shows a complex plotting of the function $G(ix; 0)$, which is nothing other than the limiting form of the well known Cole and Cole (1941) plot in the critical regime. The asymptotic expressions (18) are clearly observed on the figures. Note in particular the angle $\delta_c = \pi/4$ on the limiting Cole-Cole plot near the origin, reflecting the bulk scaling law (2) at the threshold. Our data lead to the following approximate values for the amplitudes appearing in equation (18a): $D \simeq 2.08$, $E \simeq 4.0$; the large x behaviour $\text{Re } G = -\text{Im } G = (2x)^{-1/2}$ shown in figures 2 and 3 by a broken curve is accurately observed down to $x \simeq 1$.

Consider now the finite-size scaling law (15) where *both* x and y are non-zero. The asymptotic behaviour of $\text{Re } G$ and $(-\text{Im } G)$ when $|y| \rightarrow \infty$ at *fixed* positive x is

$$y \rightarrow +\infty \quad \text{Re } G \simeq B_+ y^{-s} \quad (19a)$$

$$-\text{Im } G \simeq \frac{A}{x} y^t \quad (19b)$$

$$y \rightarrow -\infty \quad \text{Re } G \simeq B_- |y|^{-s} \quad (19c)$$

$$-\text{Im } G \simeq Cx |y|^{-2s-t} \quad (19d)$$

where the amplitudes A , B_{\pm} are identical to those of the bulk static DC conductivity

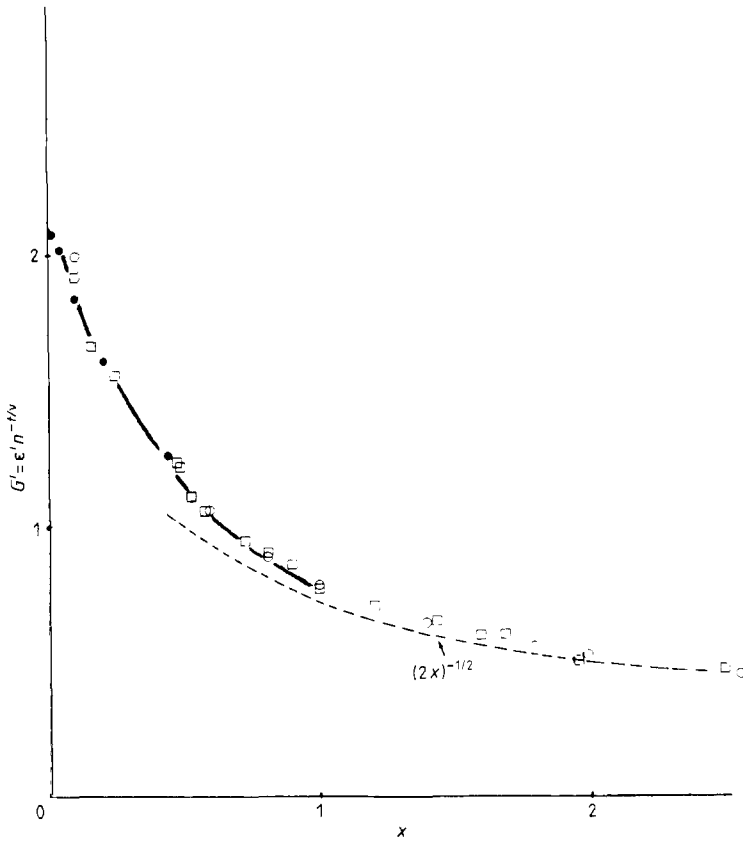


Figure 2. Plot of the real part of the scaling function $G(ix, 0)$ of the dielectric constant at the percolation threshold against x ($y=0$). The symbols denote the values of the strip width; \square , $n=6$; \circ , $n=10$; \bullet , $n=16$. The length $L \geq 10^4$ is such that statistical errors are less than the symbol height. The broken curve shows the asymptotic law (18b).

and dielectric constant:

$$\Sigma(p; \omega = 0) \approx R_0 A (p - p_c)^t \quad \text{for } p \rightarrow p_c^+ \quad (20a)$$

$$\varepsilon(p; \omega = 0) \approx C_0 B_{\pm} |p - p_c|^{-s} \quad \text{for } p \rightarrow p_c^{\pm} \quad (20b)$$

Figures 5 and 6 show plots of the real and (minus) the imaginary part of $G(ix; y)$ against y for $x=1$. A clear data collapse is still observed. The function $(-\text{Im } G)$ is monotonously increasing with y , while $\text{Re } G$ reaches a maximum $G^* \approx 0.83$ for $y = y^* \approx 0.3$.

The systematic *corrections* to the finite-size scaling law (16) are much larger for $y > 0$ than for $y < 0$, since the difference between the strips and the infinite plane is felt more drastically for $p > p_c$, where the plane possesses an infinite conducting cluster, which cannot exist on a strip. For instance, the DC conductivity of our strips is strictly zero for every finite n and every $p < 1$.

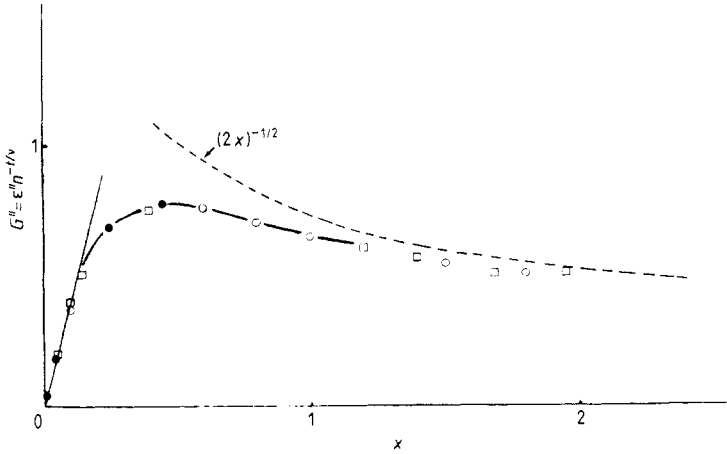


Figure 3. Same as figure 2 for minus the imaginary part of the scaling function $G(ix; 0)$.

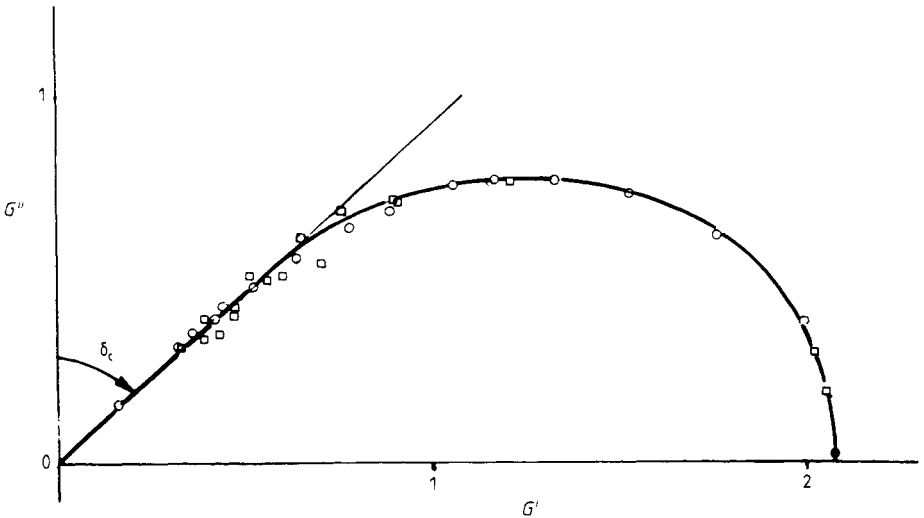


Figure 4. Complex Cole and Cole plot of the scaling function $G(ix; 0)$. The symbols read as in figure 2. Note the angle $\delta_c = \pi/4$ near the origin.

These unavoidable effects imply that more ambitious quantitative measurements, like, for instance, a good determination of the universal amplitude ratio B_+/B_- (see equations (19) and (20)) from the asymptotic behaviour (19a)-(19c) of the scaling function $\text{Re } G$, would require a considerably larger amount of computer time than we found reasonable to spend in the present work.

3.2. Various dielectric properties

Our transfer matrix approach is also an efficient tool to predict quantitatively AC properties of composite materials. We shall focus our attention on the concentration and frequency dependence of the loss angle δ and the Cole and Cole plot, keeping in

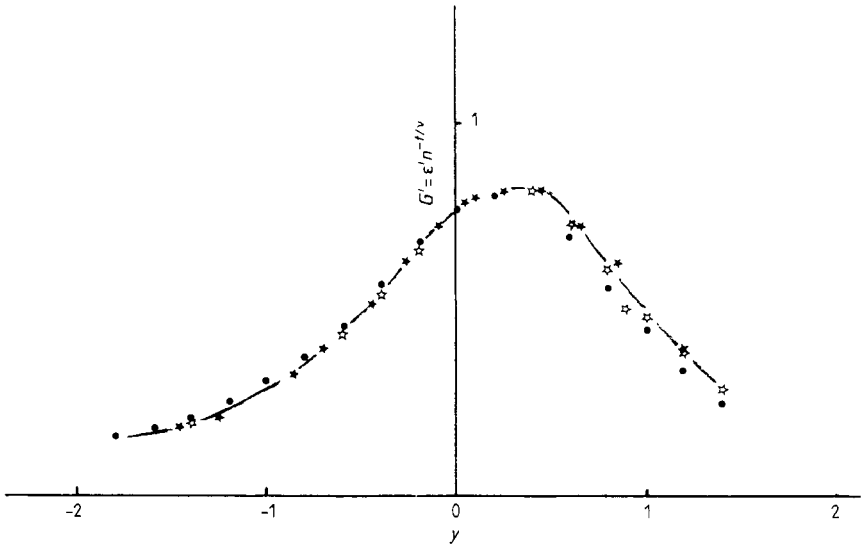


Figure 5. Plot of the real part of the scaling function $G(ix; y)$ for $x = 1$ against y . The symbols read: ●, $n = 10$; ☆, $n = 16$; ★, $n = 24$. The data have been obtained with $L \geq 10^4$. A systematic effect forbids us to get data with reasonable accuracy for $y > 1.2$ with $L = 5 \times 10^4$.

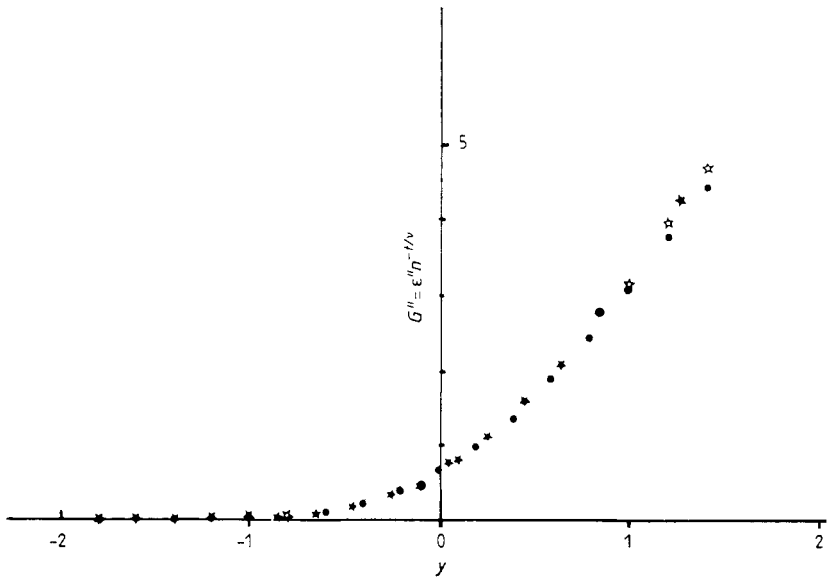


Figure 6. Same as figure 5 for minus the imaginary part of $G(ix; y)$ for $x = 1$ against y .

mind that other quantities of experimental or even industrial interest can be computed by our method without much effort.

We consider first the whole ω and p dependence of the loss angle δ , defined in equation (4). The duality identity (7a) implies that the values of Σ at frequencies ω and ω_0^2/ω have equal phases. We have therefore the following exact result, valid for

arbitrary values of p and ω :

$$\delta(p; \omega) = \delta(p; \omega_0^2/\omega). \quad (21)$$

Figure 7 shows a log-log plot of $\tan \delta$ against ω/ω_0 for different values of p , both above and below p_c . Equation (21) implies a mirror symmetry of the curves with respect to the y axis. It is clear that our algorithm can only predict accurately the properties of the 2D medium if we use a width n (much) larger than the bulk correlation length ξ . In the critical region where ξ becomes large, our data need a more refined analysis than that in § 3.1. This delicate convergence question explains why figure 7 does not show data corresponding to values of p too close to the threshold p_c . The loss angle δ exhibits the following characteristics. In the percolating phase ($p > p_c$), the presence of an infinite cluster of resistors implies that $\tan \delta$ grows as ω^{-1} for $\omega \ll \omega_0$, and hence as ω for $\omega \gg \omega_0$, thanks to the symmetry property (21). Conversely, for $p < p_c$, $\tan \delta$ vanishes like ω (resp ω^{-1}) as ω goes to 0 (resp ∞). In the critical region, $\tan \delta$ develops a plateau at the value $\tan \pi/4 = 1$, according to equations (2)–(5). These various behaviours have already been discussed in the framework of real space renormalisation (Luck 1985) and of exactly soluble fractal models (Clerc *et al* 1984, 1985); the present work is nevertheless the first approach to these properties in a realistic geometry.

The properties of the complex dielectric constant are also usefully visualised by the usual Cole and Cole plot, which has already been used in an appropriate scaling form in § 3.1. Figure 8 shows this complex plot for different values of p belonging to both phases, in units such that $R_0 = C_0 = 1$. For $p = 0$, the plot is reduced to a single point, since $\varepsilon = 1$ for all frequencies in that limit. Conversely for $p = 1$, $\Sigma = 1$ and the

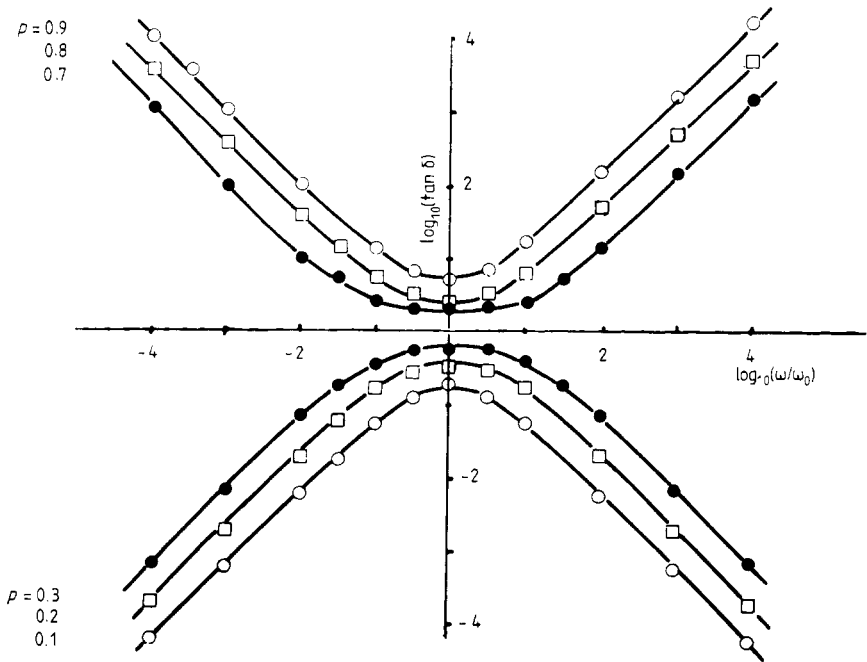


Figure 7. Log-log plot of the tangent of the loss angle δ against reduced frequency ω/ω_0 . Values of p are indicated on the curves. The different asymptotic slopes are discussed in the text.

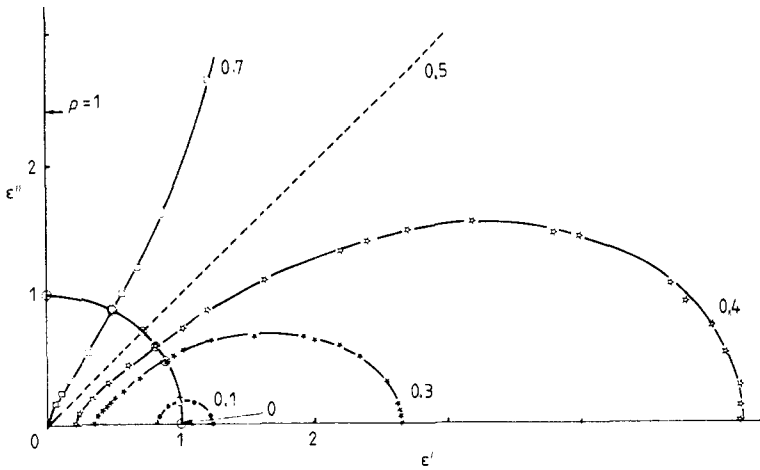


Figure 8. Cole and Cole plot of the complex dielectric constant (in units such that $R_0 = C_0 = 1$). Values of p are indicated on the curves. The straight lines ($p = p_c = \frac{1}{2}$ and $p = 1$) are exact results, as well as the quarter of a circle corresponding to $\omega = \omega_0 = 1$.

plot becomes the entire positive imaginary axis. The plot associated with the percolation threshold $p_c = \frac{1}{2}$ is also exactly known: it is a straight line defined by the angle $\delta_c = \pi/4$, because the self-duality identity (7b) implies the simple but remarkable expression:

$$\varepsilon(p_c; \omega) = C_0(i\omega/\omega_0)^{-1/2} \tag{22}$$

which is clearly valid for *all* frequencies, since it is once more merely a consequence of Straley's identities (6). For $0 < p < p_c$, the plot is generically a regular curve, intersecting twice the real axis at a right angle ($\varepsilon(\omega)$ being analytic away from the critical point). The abscissae of these intersection points are $\varepsilon(p; 0)$ and $\varepsilon(p; \infty)$; these quantities are *reciprocal* numbers, according to the identity (6). Except for very small values of p , the Cole and Cole plot is by no means close to being half a circle. For p close to p_c , the plots develop an asymptotically straight part centred around $\omega = \omega_0$, corresponding to the plateau of $\tan \delta$. The circled points represent the dielectric constant at $\omega = \omega_0$. These points are expected to lie on a quarter of a *circle*, since equation (6) implies that $|\varepsilon(p; \omega_0)|$ is equal to unity for all values of p . This provides another non-trivial check of the efficiency and accuracy of our method. For $p > p_c$, the plots extend up to infinity, since the dielectric constant diverges for $\omega \rightarrow 0$ as

$$\varepsilon(p; \omega) \sim \Sigma(p; 0)/i\omega$$

and reach the origin parallel to the imaginary axis since $\Sigma(p; \infty)$ is also a finite number.

4. Conclusion

The variety of the results obtained by the present numerical method shows that AC properties of disordered systems can be of great interest from a theoretical, experimental and industrial point of view.

The transfer matrix method of Herrmann *et al* (1984) had been shown by these authors to be one of the most efficient ways of computing the critical exponent s through DC conductivities. We have seen throughout the present paper that its

generalisation to AC phenomena provides numerous accurate results for moderate computer time, at least in two dimensions.

The analysis of our data in the critical region shows excellent agreement with the predictions of finite-size scaling theory. In particular we have obtained a satisfactory global picture of the complex scaling functions F and G .

Our study of the frequency and concentration dependence of quantities such as $\tan \delta$ and the Cole and Cole plot describes detailed properties of the resistor-capacitor model in terms of directly measurable quantities. A remarkable effect of randomness is the strong p dependence of the Cole and Cole plot and, above all, the existence of a straight region due to criticality and characterised by the universal angle δ_c (equal to $\pi/4$ in two dimensions), which also clearly appears in plots of $\tan \delta$. Two experimental groups (Laugier 1982, van Dijk 1985) have pointed out this feature, which has permitted them to interpret the electrical properties of their systems in terms of percolation models. An analogous phenomenon has been described by Le Méhauté and Dugast (1983) in electrolytes.

The extension of the present study to the three-dimensional case is by now in progress at Université de Provence. Besides its manifest experimental and industrial interest (e.g. screen-printing techniques), the three-dimensional model also provides attractive challenges for the theorist (determination of the exponent u , amplitude ratios, scaling functions).

Acknowledgments

The authors are most grateful to B Derrida for having communicated to them a version of the program used by Herrmann *et al* (1984), for his interest in the present work and for useful comments.

One of us (JPC) wishes to thank T C Lubensky for a fruitful discussion.

References

- Brézin E 1982 *J. Physique* **43** 15
 Clerc J P, Giraud G, Laugier J M and Luck J M 1985 *J. Phys. A: Math. Gen.* **18** 2565
 Clerc J P, Tremblay A M S, Albinet G and Mitescu C D 1984 *J. Physique Lett.* **45** L913
 Cole K S and Cole R H 1941 *J. Chem. Phys.* **9** 341
 den Nijs M P M 1979 *J. Phys. A: Math. Gen.* **12** 1857
 Derrida B and Vannimenus J 1982 *J. Phys. A: Math. Gen.* **15** L557
 Derrida B, Zabolitzky J G, Vannimenus J and Stauffer D 1984 *J. Stat. Phys.* **36** 31
 Efros A L and Shklovskii B I 1976 *Phys. Status Solidi* **b 76** 475
 Fisher M E 1972 *Critical Phenomena. Proc. 51st Enrico Fermi Summer School, Varenna* ed M S Green (New York: Academic)
 Herrmann H J, Derrida B and Vannimenus J 1984 *Phys. Rev. B* **30** 4080
 Laugier J M 1982 *Thèse de 3ème cycle* Université de Provence, Marseille
 Le Méhauté A and Dugast A 1983 *J. Power Sources* **9** 359
 Luck J M 1985 *J. Phys. A: Math. Gen.* **18** 2061
 Stephen M J 1978 *Phys. Rev. B* **17** 4444
 Straley J P 1976 *J. Phys. C: Solid State Phys.* **19** 783
 ——— 1977 *Phys. Rev. B* **15** 5733
 van Dijk M A 1985 *Phys. Rev. Lett.* **55** 1003
 Webman I, Jortner J and Cohen M H 1975 *Phys. Rev. B* **11** 2885
 Wilkinson D, Langer J S and Sen P N 1983 *Phys. Rev. B* **28** 1081
 Zabolitzky J G 1984 *Phys. Rev. B* **30** 4077